

## Efficient tight-binding approach for the study of strongly correlated systems

Simone Sanna,<sup>1,2,\*</sup> B. Hourahine,<sup>3</sup> U. Gerstmann,<sup>4</sup> and Th. Frauenheim<sup>2</sup>

<sup>1</sup>*Theoretische Physik, Universität Paderborn, Warburger Strasse 100, D-33098 Paderborn, Germany*

<sup>2</sup>*BCCMS, Universität Bremen, Otto-Hahn-Allee 1, 28359 Bremen, Germany*

<sup>3</sup>*SUPA, Department of Physics, University of Strathclyde, John Anderson Building, 107 Rottenrow, Glasgow G4 0NG, United Kingdom*

<sup>4</sup>*Institut de Minéralogie et de Physique des Milieux Condensés, Université Pierre et Marie Curie, Campus Bouicaut, 140 rue de Lourmel, 75015 Paris, France*

(Received 11 June 2007; revised manuscript received 14 September 2007; published 30 October 2007)

In this work, we present results from self-consistent charge density functional based tight-binding (DFTB) calculational scheme, including local-density approximation + $U$  (LDA+ $U$ ) and simplified self-interaction-corrected-like potentials for the simulation of systems with localized strongly correlated electrons. This approach attempts to combine the efficiency of tight binding with the accuracy of more sophisticated *ab initio* methods and allows treatment of highly correlated electrons for very large systems. This is particularly interesting for the case of rare earths in GaN, where dilute amount of rare earth ions is used. In this work, we show the results of test calculations on bulk ErN and on the substitutional Er<sub>Ga</sub> in wurtzite GaN, which we choose as representatives of bulk and point defects in solids with strongly correlated electrons. We find that ErN is a half metal in the ferromagnetic phase and that the substitutional Er<sub>Ga</sub> in wurtzite GaN has  $C_{3v}$  symmetry. These examples show that the DFTB approach reproduces well the results of more demanding calculation schemes with a very low computational cost, making it suitable for the study of extended systems beyond the capabilities of density functional theory.

DOI: [10.1103/PhysRevB.76.155128](https://doi.org/10.1103/PhysRevB.76.155128)

PACS number(s): 61.72.Ji, 71.20.Eh, 71.27.+a

### I. INTRODUCTION

Rare earth compounds have been a long time puzzle. They show extremely interesting properties but are quite difficult to investigate both experimentally and from the theoretical point of view. Researchers realized that even a small amount of impurities or crystal disorder could dramatically affect the properties of relatively simple systems such as rare earth (RE) monopnictides,<sup>1</sup> which were then combined with the well known problems of chemically separating different rare earths. Theorists instead had to face the problem that usual approaches for the simulation of large electronic systems, local-density approximation (LDA) or generalized gradient approximation (GGA), could not satisfactorily describe compounds with strong electron-electron interactions. A proper treatment of the strongly correlated  $4f$  electrons of the lanthanides, in fact, goes beyond a classical mean-field approach, and computational methods which are able to address this correlation problem, such as the GW approximation<sup>2</sup> or LDA extensions including orbital-dependent potential such as self-interaction correction (SIC),<sup>3,4</sup> are computationally demanding. In an attempt to improve the description of strongly correlated systems while extending the size of the studied system, different orbital-dependent corrections have been implemented in the spin-polarized charge-self-consistent density functional based tight binding (DFTB),<sup>5,6</sup> namely, the LDA+ $U$  [in both fully localized limit (FLL) and around mean field (AMF)] and a pseudo-SIC approach.<sup>7,8</sup> This gives us the possibility to treat large systems containing RE in an accurate manner within a fast tight-binding (TB) framework. At the same time, we can make a comparison of pros and cons of the different orbital-dependent approaches as well as investigating how far simple LDA-like approaches can be used to simulate  $f$  sys-

tems, in order to help elucidate whether to include the  $f$  electrons in the valence or treat them as *semicore* electrons when using standard LDA. We find that in general, as was suggested over ten years ago by Pethukov *et al.*,<sup>9</sup> including the strongly localized RE  $4f$  electrons in the core is a satisfactory approximation when  $f$  electrons are not directly involved in the bond and the ionization energy of the  $4f$  states is large in comparison with the band gap. In particular, structural properties such as lattice constants or bulk moduli are quite unaffected by the details of the method used to treat the  $4f$  orbitals. We test our methods on both a bulk RE compound and RE impurities: We choose ErN as representative of the first class of systems and Er<sub>Ga</sub> in GaN as representative of the second. Both examples are relevant for technological applications: ErN has been recently suggested as an ideal magnetic refrigerator and regenerator for cryogenic applications<sup>10,11</sup> and as basis for spin filter devices (because of its half metallicity), while Er-doped GaN samples have been successfully exploited (because of the sharp intra- $f$  optical transitions) for both the 1.54  $\mu\text{m}$  telecommunications frequency and as a primary color emitter (green) in thin film electroluminescent phosphor systems.<sup>12</sup> More generally, rare earths are also promising candidates for the realization of high  $T_c$  semiconductor spintronic devices.<sup>13,14</sup> These are also controversial systems: Pethukov *et al.*<sup>9</sup> found ErN to be a semiconductor, while Duan *et al.*<sup>1</sup> recently classified it as half metal. We present here a characterization of ErN including the electronic structure primarily in the ferromagnetic (FM) phase, finding ErN to be a half metal.

This paper is organized as follows. In Sec. II, we outline the spin-polarized self-consistent charge density functional based tight-binding (SCC-DFTB) approach and its orbitally dependent extensions (LDA+ $U$  and SIC-like). In Sec. III, we test the accuracy of the DFTB scheme for each approach implemented (deriving data to compare with experimental

measurements and *ab initio* calculations). Finally, in Sec. IV, we summarize and discuss the features of the approaches in the framework of DFTB.

## II. METHODS

### A. Density functional based tight-binding approach

Despite its simplicity (a only two-center nonorthogonal Hamiltonian is used), the density functional based tight-binding (DFTB) method scheme has been proven to be accurate when applied to solid state,<sup>15</sup> molecular, or biological systems.<sup>16</sup> Materials such as silicon,<sup>17</sup> SiC,<sup>18</sup> diamond,<sup>19</sup> boron and boron nitride,<sup>20</sup> and III-V semiconductors such as GaN (Ref. 21) and GaAs (Ref. 22) have successfully been studied within the DFTB approach.

The study of strongly correlated systems (such as RE or transition metal containing compounds) requires somewhat different techniques to the usual methods for the simulation of solid state systems because of the nature of these atoms. RE ions, for example, have atomic numbers of between 57 and 70; hence, relativistic effects become important. Additionally, many properties of transition metal or lanthanide elements depend on the strongly correlated behavior of their *d* or *f* electrons. Studying such cases requires a more sophisticated theory than simple mean-field methods. To address all of these additional complexities in treating lanthanides, the DFTB method has been substantially extended. To treat strongly correlated systems, LDA+*U*<sup>5,23</sup> and pseudo-SIC-like<sup>7,8</sup> approaches have been adopted. We would like to remark that (to our knowledge) DFTB contains the published TB implementation of LDA+*U* and SIC-like methods. The spin-polarized, charge-self-consistent DFTB approach has been extensively discussed elsewhere;<sup>6,24</sup> we briefly review the method in the Appendix for completeness and to introduce the notation used in Sec. II B.

### B. Orbital-dependent potentials

In the density functional theory (DFT), the exchange-correlation potential is often approximated by using the exchange correlation present in a homogeneous electron gas (LDA), which has been proven to be very successful for solids even if not all systems are equally well described. Materials with strongly correlated electrons, however, are examples where this mean-field approach most strikingly fails. LDA is, in fact, a one-electron method with an orbitally independent potential, and applying it to a system containing transition metals (TM) or rare earths (REs) with partially filled *d* or *f* shells gives results consistent with a metallic electronic structure and itinerant *d* or *f* electrons, which is definitely wrong for most RE compounds and several examples of TM systems (NiO being the classic example). Other choices for the exchange correlation such as generalized gradient (GGA) can also be applied, but as with LDA, this is a mean-field correction for the noninteracting system and so suffers from the same pathology. In the strongly correlated systems, the *d* or *f* electrons are often strongly localized, and there is a noticeable energy difference between occupied and unoccupied states with strong *d* or *f* character,

which are called *lower* and *upper* Hubbard bands, in analogy with the Hubbard Hamiltonian approach. There have been a number of attempts to go beyond the LDA and make it able to account for strong electron-electron correlation in such systems. The full self-interaction-corrected (SIC) approach<sup>3</sup> can reproduce the localized nature of *d* and *f* electrons in TM and RE compounds as well as the total energy of these systems but is not intended to reproduce the one-electron energies; additionally, SIC is known to overcorrect many properties.<sup>25</sup> As discussed in Sec. II E, there have also been several recent attempts to approximate the effects of the SIC method with (semi)local corrections. An alternative correction, the LDA+*U* approach, is conceptually similar to the Hubbard Hamiltonian approach: the nonlocal and energy dependent self-energy is approximated by a frequency independent but nonlocal screened Coulomb potential.

### C. LDA+*U*

As discussed by Anisimov *et al.*,<sup>26</sup> it is natural to separate electrons into localized *d* or *f* electrons and delocalized *s* and *p* electrons. While for the latter an orbitally independent one-electron potential (as in LDA) will suffice, a Hartree-Fock-like interaction better describes the local interactions of the strongly localized *d* or *f* electrons. This is of the form  $\frac{1}{2}\sum_{i\neq j}n_i n_j$ , where  $n_i$  are the occupancies of the localized shells. If we assume that the Coulomb energy of the electron-electron interaction as a function of the total number of electrons  $N=\sum n_i$  is well represented by LDA (even if it gives wrong single-particle energies), then LDA already contains part of this energy. This must be subtracted from the total energy and instead replaced with a Hubbard-model-like term. As a result, we get the functional<sup>27,28</sup>

$$E = E_{\text{LDA}} - \frac{1}{2}UN(N-1) + \frac{U}{2}\sum_{i\neq j}n_i n_j = E_{\text{LDA}} + \Delta E_{\text{LDA}+U}. \quad (1)$$

Strictly speaking, the process of subtracting the double counting of the electron-electron interaction of strongly correlated electrons from the LDA total energy and substituting it with a Hubbard Hamiltonian-like term is not without ambiguity. The electron-electron interactions have already been taken into account in a mean-field way with LDA, while the Hubbard Hamiltonian also incorporates a large part of the total Coulomb energy of the system. One can try to identify those parts of the DFT total energy corresponding to the interactions included with the Hubbard Hamiltonian in order to subtract them. This is not trivial, because while the Kohn-Sham Hamiltonian is written in terms of the total density, the Hubbard Hamiltonian is written in terms of orbital occupation numbers, and a direct link between the two is not straightforward. Secondly, even if it were possible to exactly remove the on-site Coulombic contribution in the LDA and Hartree contributions, it would be undesirable, as the spatial variation of the Coulomb and exchange-correlation potential is important and is better described in DFT than in the Hubbard approach. It is instead better to try and identify a mean-field part of the Hubbard Hamiltonian and subtract that, leaving only a correction to the LDA solution.

In the limit of uniform occupancy (all occupations equal to the average value in that shell), the corrections for total energy and potential can be written in terms of on-site occupation matrices ( $n$ ) as<sup>29</sup>

$$\Delta E^{AMF} = -\frac{1}{2} \sum_a \sum_{l \in a} (U-J)_l \sum_{\sigma} \sum_{\mu\nu} (\delta n_{\mu\nu}^{\sigma} \cdot \delta n_{\nu\mu}^{\sigma})_{\nu\mu \in l}, \quad (2)$$

$$\Delta V_{\mu\nu}^{\sigma} = -(U-J) \delta n_{\nu\mu \in l}^{\sigma}, \quad (3)$$

where  $U$  is the spherically averaged Hubbard repulsion and  $J$  is the intra-atomic exchange.  $\delta n$ , the orbital occupation matrix, is given by

$$\delta n_{\mu\nu}^{\sigma} = n_{\mu\nu}^{\sigma} - \bar{n}_{\mu\nu}^{\sigma} \delta_{\mu\nu}.$$

Here,  $\delta_{\mu\nu}$  “masks out” elements off the diagonal of the average occupation matrix  $\bar{n}_{\mu\nu}^{\sigma}$ , the effect being to return a matrix shifted by the average occupation. In the “around mean-field” (AMF) limit, the LDA+ $U$  correction to the electronic potential averaged over all occupied states is, in a given shell, zero; this is a possible way to define a mean field. For strongly correlated systems (or in the presence of a crystal and/on ligand field), the limit of uniform occupancy is not correct and the AFM functional leads to rather unrealistic results for strongly localized electrons. This has led to the suggestion of another correction which produces the correct behavior in the fully localized limit (FLL) where the eigenvalues of  $n_{\mu\nu}^{\sigma}$  are either 0 or 1,

$$\Delta E^{FLL} = -\frac{1}{2} (U-J) \sum_{\sigma} \sum_A \sum_{\mu\nu} [(n_{\mu\nu}^{\sigma})^2 - n_{\mu\mu}^{\sigma}]_{\mu\nu \in l \in A}, \quad (4)$$

$$\Delta V_{\mu\nu}^{\sigma} = -(U-J) \left( n_{\mu\nu}^{\sigma} - \frac{1}{2} \delta_{\mu\nu} \right)_{\mu\nu \in l \in A}. \quad (5)$$

AMF and FLL correct the mean-field double counting if the occupation numbers are, respectively, all equal or only 0 or 1. Most of the modern LDA+ $U$  calculations rely on one of these two functionals, although in real materials, the occupation numbers should lie between these two limits; hence, neither AMF nor FLL is strictly speaking correct for real systems, and one should therefore use an interpolation between the two limits.<sup>28</sup> However, AMF and FLL will bracket the correct values.

#### D. LDA+ $U$ -like approach in density functional based tight binding

While it has previously been suggested that for *empirical* tight binding the effects of on-site correlation can be mimicked by an empirical adjustment of symmetry resolved on-site energies,<sup>30</sup> this is problematic, for example, for low symmetry  $d$  electron systems or for  $f$  manifolds. In the RE ions of interest here, the so-called fully localized limit should be achieved [i.e., the orbital occupations of states localized within the  $4f$  manifold should either be 0 or 1 (Refs. 27 and 28)]. However, we also wish to test the AFM-like limit as well.

In the simplest rotationally invariant form of LDA+ $U$ ,<sup>31</sup> the correction to the LDA potential is of the form

$$\Delta V_{\mu\nu}^{\sigma} = -(U-J)_l (n_{\mu\nu}^{\sigma} - DC[n_{\mu\nu}^{\sigma}])_{\mu\nu \in l}. \quad (6)$$

where  $n^{\sigma}$  is the local spin occupation matrix within a given atomic manifold, and  $(U-J)$  is the screened and spherically averaged electron-electron interaction.  $DC[n]$  is the double counting term, and the two limiting cases FLL and AMF are

$$DC_{\mu\nu}^{\sigma}[n]^{FLL} = \frac{1}{2} \delta_{\mu\nu},$$

$$DC_{\mu\nu}^{\sigma}[n]^{AMF} = \frac{\text{Tr}(n_{\mu\nu}^{\sigma})}{2l+1} \delta_{\mu\nu},$$

Where  $l$  is the angular quantum number.  $(U-J)$  is usually taken to be either an adjustable parameter or from a constrained DFT calculation. We instead present a prescription for choosing  $U$  and  $J$  from atomic calculations. Since the DFTB energy aims to be a reasonable approximation to the LDA energy, it seems sensible to adopt the form of the LDA+ $U$  energy correction unchanged for DFTB. There is then the issue of how to choose the on-site occupation matrix<sup>32</sup> for a nonorthogonal basis. In the on-site case, the modification to the total energy and the DFTB Hamiltonian can be written in terms of atomic sub-blocks of the single-particle density matrix ( $\rho_{\mu\nu \in l \in A}$ ), while for the dual basis case, the occupation matrix takes the form of a generalization of Mulliken charges:

$$n_{\mu \in l \in A, \nu \in l \in A}^{\sigma} = \frac{1}{2} \sum_B \sum_{\tau \in B} (S_{\mu\tau} \rho_{\tau\nu} + \rho_{\mu\tau} S_{\tau\nu}), \quad (7)$$

where the diagonal of the resulting occupation matrices is then basis-function resolved Mulliken charges.

#### E. Pseudo-self-interaction-corrected-like approach in density functional based tight binding

Full self-interaction-corrected (SIC) LDA is relatively expensive; hence, several cheaper approximations have appeared. We adopt in DFTB an approximation of the full SIC based on the method proposed by Vogel *et al.*<sup>7</sup> and its recent refinements,<sup>8,33</sup> which is referred to as pseudo-SIC (or pSIC) as it only includes contributions near to atoms. Since the majority of the self-interaction error, in the case of interest, is local in character, this hopefully captures the majority of the error. To ensure that for single electrons the Coulomb and exchange-correlation terms are canceled out exactly, the exchange-correlation potential is modified by subtracting off the local self-interaction in this basis:

$$\Delta V_{\mu, \text{pSIC}}^{\sigma} = -\alpha V_{\mu, H+XC}^{\sigma}[n_{\mu}(\mathbf{r}), m_{\mu}(\mathbf{r})]. \quad (8)$$

To make calculations of the potential tractable,  $V_{H+XC}$  is approximated as that for a single, fully occupied and completely spin-polarized state  $V_{H+XC}^{\sigma}[n(\mathbf{r}), m(\mathbf{r})] = V_{H+XC}^{\sigma}[1, 1]$ . The prefactor  $\alpha$  allows an additional scaling of the potential, for example, to account for electronic relaxation on electron removal ( $\alpha = \frac{1}{2}$  in the work of Filippetti and Spaldin; however, this is incorrect for a system with a single electron<sup>33</sup>). As yet, no energy expression related by variational principle

to the potential is available;<sup>8,33</sup> hence, no expression for interatomic forces has been derived. In the following, we will derive such an expression from similarities between the LDA+ $U$  and pSIC formalism. Equation (8) is not invariant to unitary transforms; however, similar to the original LDA+ $U$  formalism,<sup>23</sup> this can be achieved by using the density matrix formulation,

$$\Delta V_{\text{pSIC}}^{\sigma} = -\alpha V_{H+\text{XC}}^{\sigma}[1,1]n_{\mu\nu}^{\sigma}. \quad (9)$$

Considering, as previously, a fully occupied and completely spin-polarized state, we can write (due to the similarity in the functional of the potential to LDA+ $U$ ) in matrix form an energy expression (which is directly connected to the potential) as

$$\Delta E^{\text{pSIC}} = -\alpha \sum_{\sigma} V_{H+\text{XC}}^{\sigma}[1,1] \text{Tr}(n^{\sigma} \cdot n^{\sigma}). \quad (10)$$

In these approximations, pSIC is written as a type of non-double counted LDA+ $U$  [i.e.,  $DC[n]$  is absent from Eq. (6)], without ambiguity in the choice of  $(U-J)$ , since the prefactor comes from the exchange-correlation potential. Additionally, atomic forces can be derived.<sup>32</sup> This has some similarity to the atomic SIC (or ASIC) form of Pemmaraju *et al.*,<sup>33</sup> however, they do not provide a variationally connected energy.

#### F. Connection between LDA+ $U$ and pseudo-self-interaction-corrected

In the following, we will discuss a connection between LDA+ $U$  in its FLL version and pSIC that allows a further simplification of the latter approach in a tight-binding scheme. The starting point of this discussion is Eq. (44) of Anisimov *et al.*,<sup>26</sup> relating the atomic Slater integral  $F^0$  and the exchange  $J$  to the LDA potential for an atomic state as

$$V_{H+\text{XC}}^{\sigma} = F^0 N - \frac{1}{2}(F^0 - J) - JN_{\sigma}. \quad (11)$$

Thus, for the orbital occupation choices for which  $V_{H+\text{XC}}$  is needed in pSIC ( $V_{H+\text{XC}}[1,1]$ , i.e.,  $N=N_{\sigma}=1$ ), the spherically symmetric part of the exchange-correlation potential is given by

$$V_{H+\text{XC}}^{\sigma}[1,1] = \frac{F^0 - J}{2}.$$

In DFTB, we use  $U$  in the SCC-DFTB correction (see the Appendix) that is related to the screened  $F^0$  Slater integral.<sup>26</sup> If we, moreover, assume in the zeroth limit that screening in the isolated atom, for which  $U$  is calculated, is small,  $F^0$  can be substituted by  $U$ . Similarly, the diagonal part of the spin coupling matrix  $W_{ll'}\delta_{ll'}$ , given in the Appendix, is equivalent to  $J_l$ . We thus obtain, for the basis that is used to expand the local states in pSIC,

$$V_{H+\text{XC}}^{\sigma}[1,1] \approx \frac{(U-J)_{\text{atomic}}}{2}. \quad (12)$$

In this approximation, pSIC then gives a contribution to the potential of

$$(\text{pSIC})\Delta V_{\mu\nu}^{\sigma} = -\alpha \frac{(U-J)_{\text{atomic}}}{2} n_{\mu\nu}^{\sigma}. \quad (13)$$

For a system with a Hubbard gap, the relaxation-corrected form of pSIC ( $\alpha=\frac{1}{2}$ ) would apply the same potential to the lower Hubbard band as obtained by a FLL-LDA+ $U$  contribution of

$$(\text{FLL})\Delta V_{\mu\nu}^{\sigma} = -\frac{(U-J)_{\text{atomic}}}{2} \left( n^{\sigma} - \frac{1}{2} \right). \quad (14)$$

Since the eigenvalues of the  $n^{\sigma}$  matrix are either 0 or 1, the occupied states in the local manifold experience a net downward shift of  $-\frac{(U-J)_{\text{atomic}}}{4}$ . This suggests, in comparison with Eq. (5), that the LDA+ $U$  and relaxation-corrected pSIC have the same effect on the occupied band structure and that  $(U-J) = \frac{(U-J)_{\text{atomic}}}{2}$  is a sensible first choice for the parameters in LDA+ $U$ . This agrees with the (empirical) choice of  $\approx 0.5 \times (U-J)_{\text{atomic}}$  being suitable for many LDA+ $U$  applications.<sup>26,29</sup> Since there are different potentials for unoccupied states in pSIC and FLL-LDA+ $U$ , these methods give different gaps,<sup>33</sup> and different total energy corrections [compare Eqs. (4) and (10)].

All of the above corrections share the feature that they are semilocal (decaying on the length scale of the overlap matrix in the dual basis form); hence, they cannot fully address nonlocal effects such as the derivative discontinuity in Kohn-Sham theory.<sup>34,35</sup>

### III. RESULTS AND DISCUSSION

#### A. ErN

ErN is a good test system for our methods because it is a standard representative of a class of materials (the RE mononictides) which have attracted much recent attention due to their peculiar characteristics. Particularly interesting is the fact that despite their simple rock salt structure (common to most of the RE mononictides), the RE-N compounds show a variety of electrical and magnetic properties,<sup>9</sup> including ferromagnetic behavior, extremely low Curie and Néel temperatures, and an unusual  $\langle 111 \rangle$  spin orientation. Their suitability for epitaxial growth on several semiconductors has made them interesting materials for the realization of electronic and spintronic devices. ErN has not been as extensively investigated as other Er pnictides (such as ErAs) or other RE nitrides (such as GdN), but there is a substantial set of experimental data in the literature (see Refs. 10 and 11 and references therein) as well as several theoretical investigations<sup>1,9,36-38</sup> of this material. It is only recently<sup>1,36</sup> that a consensus has been reached about its half-metallic character, i.e., ErN shows a finite density of states at the Fermi level for one spin channel and a zero density of states for the other. In some earlier works,<sup>37</sup> ErN was described as a metal, while in others,<sup>9</sup> it was found to be a semiconductor in both ferromagnetic and paramagnetic (PM) phases. Unlike the other Er pnictides, in the ground state, ErN is a ferromagnet with a magnetic transition at 3.4–6 K.<sup>39,40</sup>

We investigated the FM and the PM magnetic phases. While it is clear that using a primitive ErN cell a spin-

polarized calculation will be a sensible representation of the FM phase (or the saturation limit of the PM phase in a magnetic field), to simulate the PM phase we adopt a crude virtual crystal approximation. Following the considerations of Pethukov *et al.*,<sup>9</sup> we consider a non-spin-polarized calculation as representative of the paramagnetic phase. This is a very drastic approximation; a proper treatment of the PM phase would require the consideration of thermal fluctuation effects and knowledge of the magnetic phase diagram. However, this approximation gives us the possibility to compare our results with literature<sup>9</sup> and suffices for the goal of this work, which is to present our methods.

We find the difference in the cohesive energy (defined as energy difference of free Er and N atoms in their spin polarized state) of the PM and FM phases to be, independent of the particular calculation approach, about 0.5 eV per atom, which is somewhat higher than the difference reported by Pethukov *et al.*<sup>9</sup>

Like other RE nitrides ErN is<sup>9,36</sup> characterized by ionic bonding; however, the equilibrium distance<sup>41</sup> (2.432 Å) of Er and N in the compound is only 0.1 Å longer than the sum of the covalent radii of Er (1.57 Å) and N (0.75 Å). The Er ions in ErN are trivalent, existing in the +3 oxidation state, corresponding to an outer electronic configuration for the Er ions of [Xe] 4*f*<sup>11</sup>, with a full *f* semishell containing seven spin up electrons and an half filled *f* semishell containing four spin down electrons. This was verified with all spin-resolved approaches implemented in DFTB. Eleven of the 12 *f* electrons remain strongly localized while the remaining one is delocalized, in agreement with the results of Temmerman *et al.*<sup>42</sup> who predict the existence of two kinds of *f* electrons, localized and delocalized, whose relative numbers change depending on the RE.

All ErN calculations in this work were performed using the rocksalt primitive cell and a 12×12×12 Monkhorst-Pack *k*-point mesh.<sup>43</sup> The *U* in the LDA+*U* approach is not considered as a free parameter as in our earlier work.<sup>44</sup> As discussed in Sec. II F, we use half of the atomic *U*–*J* value of the Er 4*f* shell. *U* and *J* were calculated for the atom using Janak's theorem. The *U*–*J* value of 7.6 eV we use is consistent with that used in similar simulations.<sup>45</sup> The +*U* potentials are applied only to the *f* shells.

We start our ErN characterization with the determination of the lattice parameter. It is interesting to see how this is influenced by different methods. As the LDA-like approach in DFTB already gives relatively accurate results for ErN, one expects LDA+*U* to overestimate the ErN lattice constant. This is verified, even if the difference between LDA and LDA+*U* is less than 2% of the lattice constant (See Table I).

In the same table, reported are the values of the bulk moduli and their first derivative (with respect to the pressure) calculated with different approaches. The values we have are, on average, slightly larger than that calculated by Pethukov *et al.*<sup>9</sup> but still within the typical error of the DFTB method. We observe that the application of the AMF and FLL approaches leads to a great improvement in the description of the bulk modulus (and a small worsening in the description of the lattice constant), while the pSIC approach improves the description of the bulk modulus without loss of

TABLE I. Lattice constants and elastic parameters calculated with the different approaches implemented in DFTB for the FM phase of ErN. Dev. stands for the deviation of the calculated from the experimental value.

Method	Lattice constant (Å)	Dev. (%)	<i>B</i> (GPa)	<i>B'</i>
Expt.	4.839 <sup>a</sup>		220.25 <sup>9</sup>	4.3
DFTB	4.895	1.1	272.14	3.5
DFTB+ <i>U</i> FLL	4.969	2.7	231.40	4.7
DFTB+ <i>U</i> AMF	4.919	1.7	224.02	6.7
DFTB pSIC	4.892	1.1	264.20	3.0

<sup>a</sup>Reference 41.

precision in the description of the lattice constant. The calculated values for the first derivative of the bulk modulus, which is a delicate parameter for both theoretical simulation and experiment, are around the experimental value for all the approaches. While the calculated values of the bulk modulus come close to the experiment with the application of orbital-dependent potentials, it does not seem to lead to major advantages in the description of *B'*.

As already mentioned, ErN is ferromagnetic in the ground state, and the results reported here are for this magnetic phase. The local (spin) density approximation [L(S)DA]-like picture is not adequate for the simulation of ErN as it shows the narrow bands deriving from the *f* states pinned at the Fermi level, which is incorrect for this material. Orbital-dependent approaches such as DFTB+*U* (both in the AMF and FLL limits) instead find ErN in the FM phase to be a half metal, in agreement with Aerts *et al.* and Duan *et al.* (see Fig. 1). As in the previously mentioned works, the paramagnetic phase has been simulated by the spin unresolved LDA+*U* approach: in this case, in both the AMF and FLL limits, ErN is then a narrow-gap semiconductor.

## B. Substitutional Er<sub>Ga</sub>

As a further test application to check the validity of our calculational methods, we chose to investigate in some detail the Er substitutional RE<sub>Ga</sub> in hexagonal (wurtzite) GaN, paying particular attention to the density of states (DOS) and stressing the differences between a classic LDA-like and the LDA+*U* approach. Er<sub>Ga</sub> can be used for testing since the RE<sub>Ga</sub> substitutionals are the simplest stable lanthanide defects in GaN and have been already studied both experimentally and theoretically.<sup>46–48</sup> Er:GaN based light emitting diodes<sup>49</sup> have stimulated many experimental attempts to understand<sup>58</sup> the mechanisms underlying the emission from Er-doped samples and to exploit<sup>51–53</sup> and improve<sup>54,55</sup> the emission itself. From experimental studies, we know that Er ions in GaN prefer the Ga position,<sup>56</sup> occur in 3+ valence state<sup>49</sup> and possess *C*<sub>3*v*</sub> symmetry<sup>57</sup> with relatively short distances to the surrounding N ligands.<sup>58</sup>

We first discuss the geometry of the defect. Two DFTB-parameter sets have been created for the simulation of RE in GaN: in one, the Ga 3*d* orbitals are treated as valence and in the other, as core. We report here results obtained not includ-

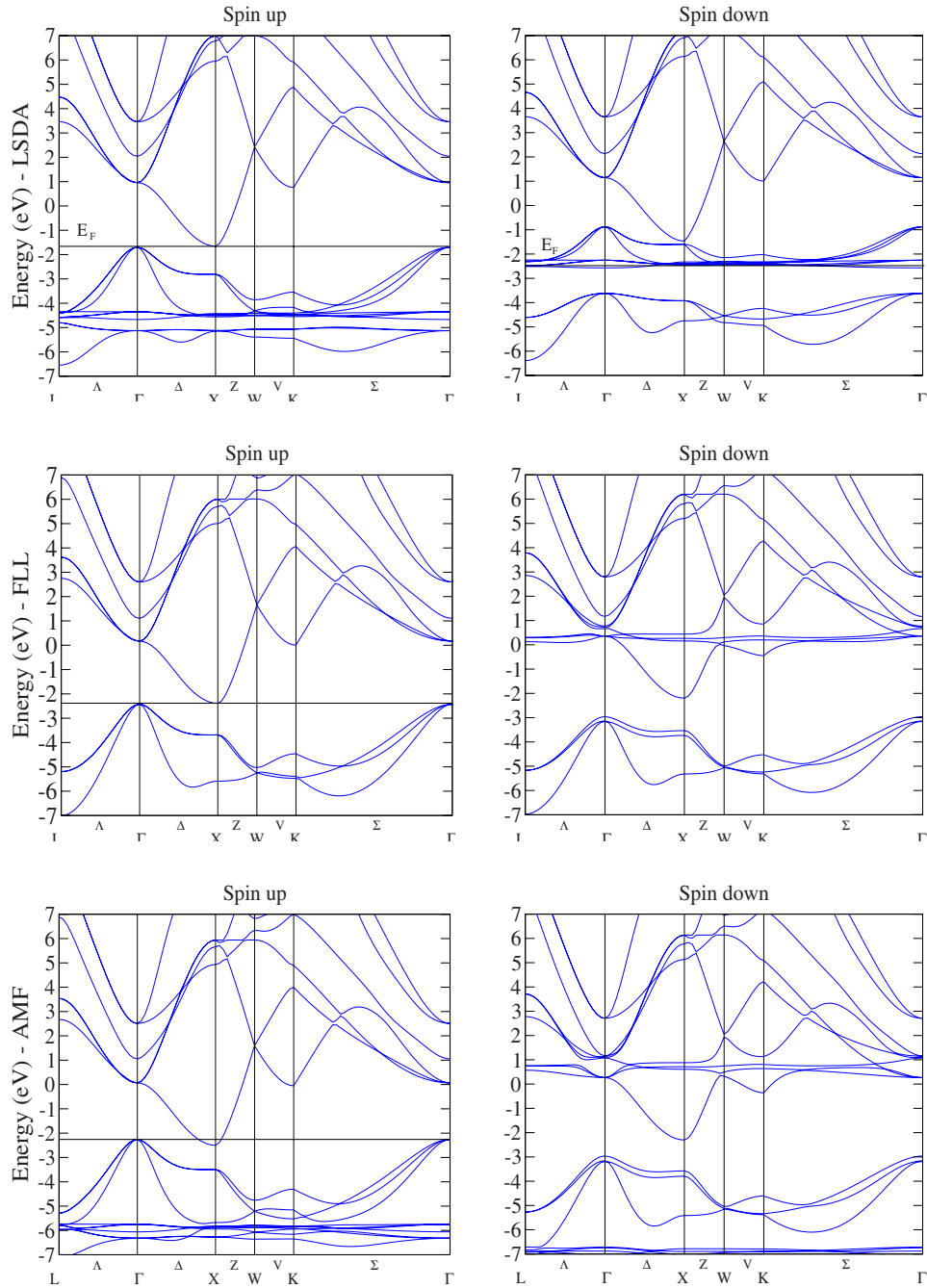


FIG. 1. (Color online) Spin-resolved band structure of rocksalt ErN calculated with the SDFTB (first row) and SDFTB+ $U$  FLL and SDFTB+ $U$  AMF (second and third rows) approaches.

ing the Ge  $3d$  in the valence. Results obtained including the Ga  $3d$  orbitals do not differ substantially and have been reported in a previous publication.<sup>59</sup> Supercells containing 256 atoms and a  $4 \times 4 \times 4$  Monkhorst-Pack  $k$ -point sampling were used to calculate the data reported here. The supercells have been relaxed in different spin configurations to find out the one that minimizes the total energy. The substitutional  $\text{Er}_{\text{Ga}}$  is found to have the  $C_{3v}$  symmetry. The Er ion is, in fact, surrounded by four N atoms, one (identified by the label  $\text{Er-N}_1$  in the Table II) being slightly more distant from the Er ion than the other three ( $\text{Er-N}_1$  in the Table II). According to

the  $C_{3v}$  symmetry, the Er second neighbors can be similarly divided in two groups (called  $\text{Er-Ga}_1$  and  $\text{Er-Ga}_2$  in Table II). The symmetry is a particularly important parameter in the investigation of the RE defects, both because it can be measured experimentally and also because it is known that the intensities of intra- $f$  transitions are enhanced by lowering the symmetry. For example, the symmetry difference between Eu and Tb substitutionals in GaN is believed to be the cause of the higher relative luminescence intensity of Eu-doped GaN, as suggested by Bang *et al.*<sup>60</sup> We find that the Er substitutional, after geometry optimization, sits on-site; the cal-

TABLE II. Bond lengths ( $\text{\AA}$ ) and local strain around the  $C_{3v}$   $\text{Er}_{\text{Ga}}$  substitutional in hexagonal GaN. For the definition of the entries in the table, see text. The local strain is defined as the ratio between the  $\text{Er-N}_1$  bonds and the  $\text{Ga-N}_1$  bonds in the bulk. For further details, see the individual references.

	$\text{Er-N}_1$	$\text{Er-N}_2$	$\text{Er-Ga}_1$	$\text{Er-Ga}_2$	Strain (%)
DFT <sup>a</sup>	2.13	2.16	3.22	3.26	
Expt. <sup>b</sup>	2.17	2.17	3.26	3.26	
DFTB	2.15	2.17	3.32	3.35	11.6
DFTB+ $U$ FLL	2.18	2.20	3.28	3.38	13.1
DFTB+ $U$ AMF	2.17	2.19	3.29	3.37	12.6
pSIC DFTB	2.17	2.18	3.29	3.36	12.6

<sup>a</sup>Reference 46.

<sup>b</sup>Reference 50.

culated geometry in the neighborhood of the substitutional is reported in Table II together with experimental measurements and other theoretical results. The calculated values are in good agreement with the experimental measurements, and the lattice distortion has values very close to previous pseudopotential LDA calculations.<sup>46</sup> Different orbital-dependent calculation schemes do not really influence the system geometry. Apart from the relatively small compressive stress in the neighborhood of the defect [Er is a bigger ion than Ga with covalent (3+ ionic) radii of 1.57 (1.03) and 1.26 (0.62)  $\text{\AA}$ , respectively], no other effects on the host geometry are observed. The compressive stress, estimated by the ratio between the Er-N bonds and the Ga-N bonds in the bulk, is reported in the last column of Table II. Already the classic LDA formulation of the DFTB approach provides Er-N bond lengths in good agreement with experimental data. The LDA+ $U$ , like and pSIC implementations, leads to small changes only. In other words, relaxing the structure with or without the contributions of the orbital-dependent potentials anyway does not substantially change the geometry of the system and influences only slightly the bond lengths: Bond lengths calculated with and without the orbital-dependent potentials differ at most by 0.03  $\text{\AA}$  (see Table II).

Let us consider now the electronic properties of the Er substitutional. We report here, for convenience, only results obtained with the FLL approach. The substitutional  $\text{Er}_{\text{Ga}}$  is a representative example, because all of the midseries RE substitutionals behave in a similar way. Reference calculations were executed with the *ab initio* all electron code WIEN2K.<sup>61</sup> In the Fig. 2, the band structures of the substitutional  $\text{Er}_{\text{Ga}}$  calculated with DFTB and DFT are reported. With LSDA/spin-DFTB (SDFTB), the GaN original band gap (3.5 eV in DFTB, 2.2 eV in WIEN2K) remains more or less unchanged on addition of the RE, while in the middle of the gap, there appears a group of very localized  $f$ -related levels. As with ErN, these levels are filled with seven up and four down electrons, which are considered to be trivalent in comparison with the isolated atomic occupations. The corresponding DOS is reported in Fig. 3 where the DFTB calculations appear on the upper part, while the WIEN2K reference calculations are reported for comparison in the lower part. For convenience, data reported in Figs. 2 and 3 were calculated using smaller 72-atom supercells.

When we apply the + $U$  potential (see Figs. 3 and 4) to the  $f$  shell, the occupied states are pushed downward into the valence band and the empty states are pushed upward into the conduction band, leaving the original band gap completely empty. A detailed discussion about the interpretation of this clear gap can be found in Ref. 62 and references therein. The DOS changes are consistent with what is observed for the band structure: The  $f$ -related peak in the band gap is removed, leaving the GaN band gap free again. This is in agreement with the paper of Filhol *et al.*,<sup>46</sup> where they found that simple RE substitutionals do not induce localized states in the band gap (in their case, they investigated this only for non- $4f$ -related states, however). In Fig. 4, the DOSs for the studied system calculated with WIEN2K and with DFTB are shown to be in very good agreement. In this situation, a simple LDA-like approach treating the  $f$  electrons as corelike electrons produces the same results of a more sophisticated approach with a physical handling of the  $f$  electrons.

In Fig. 4, we also report the DOS calculated with the pSIC approach as implemented in DFTB. The pSIC poten-

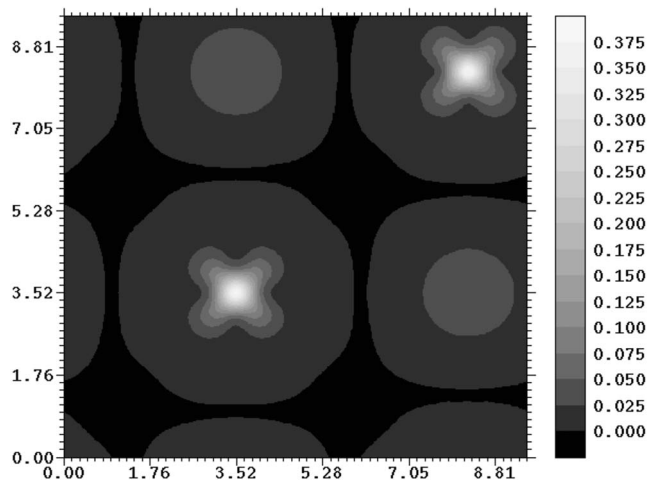


FIG. 2. Volume slice of the magnetization density in the (100) plane of rocksalt ErN in the ferromagnetic phase. The axis labels are expressed in  $\text{\AA}$  and the hue (in arbitrary units) the electronic density. The unpaired electrons are localized on the Er atoms.

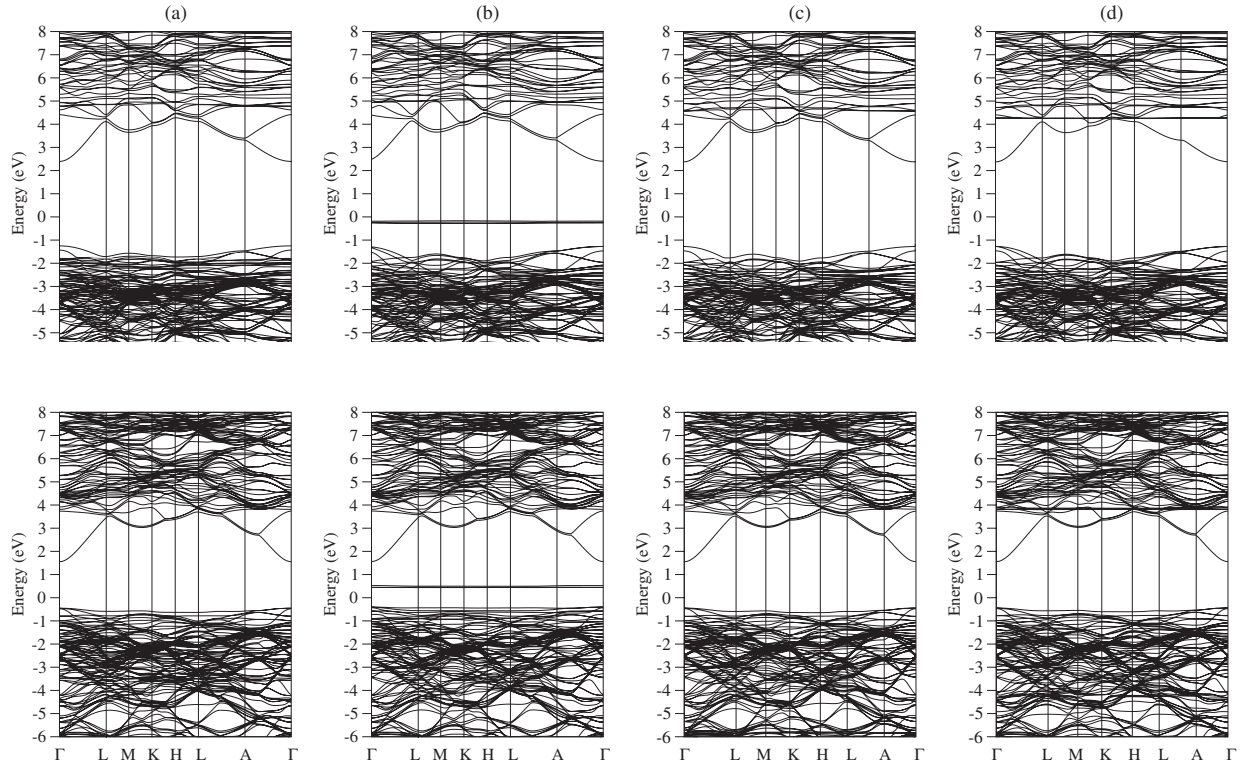


FIG. 3. The substitutional  $\text{Er}_{\text{Ga}}$  in wurtzite GaN. Spin-resolved [(a) and (c)] spin up and [(b) and (d)] spin down energy band structure calculated with [(a) and (b)] LDA/DFTB and LSDA+ $U$  [(c) and (d)] calculated with a value of  $(U-J)$  of 7.6 eV. In the first row, reported are the DFTB calculations, and in the second, WIEN2K calculations (with the same computational parameters) are reported for comparison.

tials shift occupied states downward but do not act on the empty ones. If we apply the pSIC potentials only on the  $f$  shells (similar to the usual LDA+ $U$  treatment), the shift of the occupied  $f$  states is the same as in FLL, as already expected by Eqs. (13) and (14), whereas the positions of the unoccupied states remain unchanged. However, SIC is usually applied to all occupied orbitals, as shown in the second box in Fig. 3. In this case, due to the interactions of all the SIC-corrected states, the splitting between occupied and unoccupied  $f$  levels is reduced. Furthermore, the unoccupied  $f$  states are slightly shifted to higher energies.

So far, we have neglected in our discussion the effects of spin-orbit coupling; however, we have also carried out provisional calculations in the case of Er using the methodology outlined in Ref. 77 in addition to the LDA+ $U$ -like treatment for DFTB. Using spin DFTB and a  $4f$  spin-orbit constant of  $2234 \text{ cm}^{-1}$ , with the Er magnetic moment in the  $a$  plane,<sup>63</sup> we find that the sevenfold degenerate localized gap levels shown in Fig. 2 in the gap are split into four filled and three empty nondegenerate levels which remain in the gap spanning a range of  $\sim 700 \text{ meV}$ . Applying the FLL-LDA+ $U$  approach and the same constant for the spin-orbit splitting ejects these states from the gap, demonstrating that in this case correlation has a larger effect than spin-orbit coupling. The possibility of acceptor or donor states was not investigated in this work, since all calculations were performed with neutral supercells.

#### IV. SUMMARY

We have presented a parametrization for the simulation of RE doping in GaN in the framework of the SCC-DFTB. The capability of this method to perform spin-polarized calculations and to treat strongly correlated systems with LDA+ $U$ -like approaches makes DFTB a powerful tool for the simulation of RE systems as well as other strongly correlated systems. The DFTB Er/Ga/N parametrization was tested for two different systems, RE nitrides and the substitutionals  $\text{Er}_{\text{Ga}}$  in GaN. Properties such as geometries, band structures, and density of states were tested against experimental measurements and DFT calculations and show good agreement between our simulations and existing data. The accuracy of the parameters and the efficiency of this method allow the investigation of extended systems and the systematic sampling of many configurations for defect physics and chemistry.

#### ACKNOWLEDGMENTS

This work was partially funded by the European Commission through the RENiBEL (Rare Earths Doped Nitrides for High Brightness Electroluminescence Emitters) Network (Contract No. HPRN-CT-2001-00297). The authors thank Bálint Aradi and Christof Köhler (Universität Bremen) for the technical support and useful discussion about the parametrization process, Th. Gallauner (Technische Universität



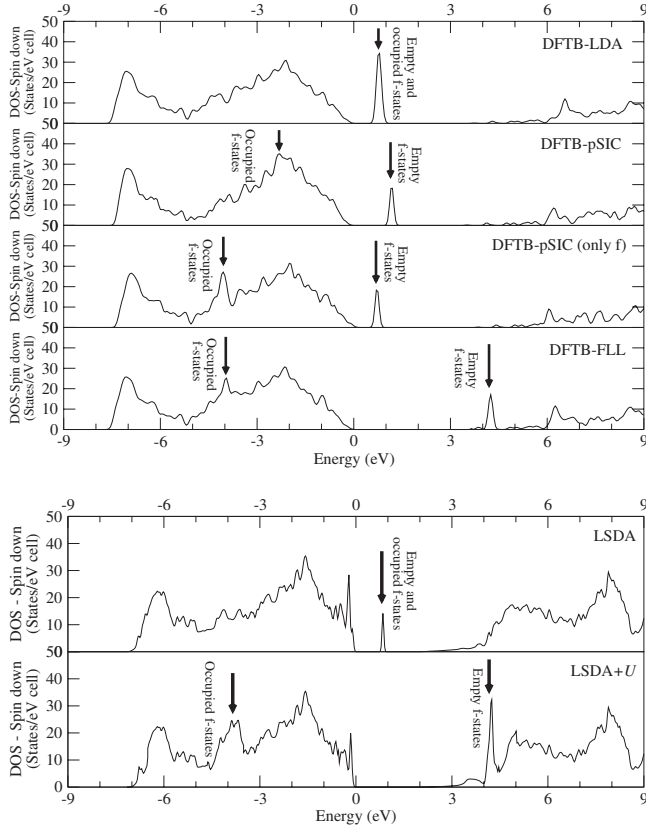


FIG. 4.  $\text{Er}_{\text{Ga}}$  in the neutral charge state in wurtzite GaN. Spin-resolved DOS calculated with the different approaches implemented in DFTB (upper box) and with LDA and LSDA+ $U$  as implemented in WIEN2K (lower box). The arrows show the position of the  $f$ -related peaks. We only show the spin down electrons, as the spin up are occupied and included in the valence band. In the LDA+ $U$  and pSIC calculations, the  $f$ -related peak visible in the band gap is split into two parts, and the rest of the structure remains almost untouched. The valence band maximum was chosen in each case as zero of the energy scale.

Wien) for the WIEN2K calculations, and Knut Vietze (Technische Universität Dresden) for making available the atomic code RLCAO. B.H. gratefully acknowledges the Royal Society of Edinburgh for funding.

#### APPENDIX: SPIN-POLARIZED DENSITY FUNCTIONAL BASED TIGHT BINDING

In the SCC-DFTB approximation, the expression for the total energy of a system of  $M$  atoms in the Kohn-Sham<sup>64,65</sup> (KS) formulation of the spin DFT is expressed expanding the charge density  $n(\mathbf{r})$  around a reference charge density of  $n_0(\mathbf{r})$ :

$$n(\mathbf{r}) = \sum_{\sigma=\uparrow,\downarrow} \sum_i^N n_{i,\sigma} |\psi_{i,\sigma}|^2 = n_0(\mathbf{r}) + \delta n(\mathbf{r}), \quad (\text{A1})$$

with  $\delta n(\mathbf{r})$  being the difference between the reference charge density used in parametrization and the charge distribution in the system. The system magnetization is also expanded around the spin-unpolarized atomic case which has (per definition) a magnetization density of zero:

$$m(\mathbf{r}) = m_0(\mathbf{r}) + \Delta m(\mathbf{r}) \quad \text{with } m_0 = 0. \quad (\text{A2})$$

Introducing the abbreviations  $n$ ,  $n_0$ ,  $\Delta n$ , and  $\Delta m$  for  $n(\mathbf{r})$ ,  $n_0(\mathbf{r})$ ,  $\Delta n(\mathbf{r})$ , and  $\Delta m(\mathbf{r})$  and with a little algebra, the expression for the DFTB total energy of the system is written as

$$\begin{aligned}
 E_{tot} = & \sum_{\sigma=\downarrow,\uparrow} \sum_i^{occ} n_{i\sigma} \langle \psi_{i\sigma} | \underbrace{-\frac{\nabla^2}{2} + v_{ext} + \int \frac{n'_0}{|\mathbf{r}-\mathbf{r}'|} d^3r' + v_{xc}[n_0, 0]}_{\hat{H}_0[n_0, 0]} | \psi_{i\sigma} \rangle \\
 & + \underbrace{E_{NN} + E_{xc}[n_0, 0] - \int v_{xc}[n_0, 0] n_0 d^3r - \frac{1}{2} \iint \frac{n_0 n'_0}{|\mathbf{r}-\mathbf{r}'|} d^3r d^3r'}_{E_{rep}} \\
 & + \underbrace{\frac{1}{2} \iint \left( \frac{1}{|\mathbf{r}-\mathbf{r}'|} + \frac{\delta E_{xc}}{\Delta n \Delta n'} \Big|_{n_0, 0} \right) \Delta n \Delta n' d^3r d^3r'}_{E_{\delta n}} + \underbrace{\frac{1}{2} \int \frac{\delta^2 E_{xc}}{\delta m^2} \Big|_{n_0, 0} \Delta m^2 d^3r}_{E_{\delta m}}
 \end{aligned} \quad (\text{A3})$$

as explained in Ref. 66. In this equation,  $\hat{H}_0[n_0, 0]$  and  $E_{rep}$  only depend on the reference density, while  $E_{\delta n}$  and  $E_{\delta m}$  include fluctuations of the charge and magnetization densities.

### 1. Zeroth-order Hamiltonian

The zeroth-order Hamiltonian contribution to this expression ( $\hat{H}_0[n_0, 0]$ ) is derived expanding the spin orbitals of the reference system as a linear combination atomic orbitals:

$$|\psi_{i\sigma}\rangle = \sum_{\nu} c_{\nu i\sigma} |\varphi_{\nu}(\mathbf{r} - \mathbf{R}_A)\rangle, \quad \nu \in A. \quad (\text{A4})$$

The basis function  $\varphi_{\nu}(\mathbf{r} - \mathbf{R}_A)$  is centered on the atomic nucleus  $A$ , with position  $\mathbf{R}_A$ . The spin is included in the coefficients  $c_{\nu i\sigma}$  of the expansion. The basis functions  $\varphi_{\nu}(\mathbf{r})$  are themselves a linear combination of Slater orbitals. The coefficients of the expansion are calculated from neutral, spin-unpolarized, and spherically symmetric *pseudoatoms*, which are described by a modified relativistic single atom Dirac equation<sup>67</sup> and to which an additional harmonic confining potential is added. Inserting Eq. (A4) into Eq. (A3), we can derive

$$\langle \psi_{i\sigma} | \hat{H}_0[n_0, 0] | \psi_{i\sigma} \rangle = \sum_{\mu, \nu} c_{\mu i\sigma}^* c_{\nu i\sigma} \hat{H}_{\mu\nu}^0[n_0, 0], \quad (\text{A5})$$

where the Hamiltonian matrix elements are calculated only for the valence electrons in a minimal basis within a two-center approximation. Neglecting crystal field and three center terms,

$$H_{\mu\nu}^0 = \begin{cases} \varepsilon_{\mu}^{\text{free atom}} & \text{if } \mu = \nu \text{ and } A = B \\ \langle \varphi_{\mu}^A | T + V_A^0 + V_B^0 | \varphi_{\nu}^B \rangle & \text{if } A \neq B \\ 0 & r > r_{\text{cutoff}}, \end{cases} \quad (\text{A6})$$

where the  $\varepsilon_{\mu}$  are the eigenvalues of the (uncompressed) atomic Kohn-Sham orbitals,<sup>68</sup> and  $V_{\text{eff}}$  is the effective Kohn-Sham potential (Coulombic plus exchange correlation) for atoms  $A$  and  $B$ .<sup>69</sup> The Hamiltonian  $\hat{H}_{\mu\nu}^0$  and overlap matrix elements ( $S_{\mu\nu} = \langle \varphi_{\mu} | \varphi_{\nu} \rangle$ ) are calculated only once and tabulated as function of the interatomic distance between  $A$  and  $B$ . Then, by following the method of Slater and Koster<sup>70</sup> and its extension to the  $f$  shell,<sup>71,72</sup> this is used to generate the two-center  $H^0$ . The values of the matrix elements in each particular calculation are computed by interpolating the tabulated data.<sup>73</sup>

### 2. Fluctuation dependent contributions to the energy

It has been shown<sup>66,74</sup> that using the Mulliken charges,

$$q_{Al\sigma} = \frac{1}{2} \sum_{i=1}^{\text{occ}} n_{i\sigma} \sum_{\mu \in A, l} \sum_{\nu} c_{\mu i\sigma}^* c_{\nu i\sigma} S_{\mu\nu}, \quad (\text{A7})$$

to write the charge density fluctuations as sum of atomic contributions compared to a reference charge distribution ( $q^0$  which is chosen from the limiting isolated atomic case),

$$\Delta q_{Al} = \left( \sum_{\sigma=\uparrow, \downarrow} q_{Al\sigma} \right) - q_{Al}^0 \quad (\text{A8})$$

(where  $l$  labels the orbital,  $A$  the atom, and  $\sigma$  the spin), the term in  $E_{\delta n}$  [Eq. (A3)] can be written (in an  $l$ -shell resolved<sup>24</sup> monopole approximation) as

$$E_{\delta n} = \frac{1}{2} \sum_A \sum_B \sum_{l \in A} \sum_{l' \in B} \Delta q_{Al} \Delta q_{Bl'} \gamma_{Al, Bl'}, \quad (\text{A9})$$

where  $\gamma_{Al, Bl'}$  is an analytical<sup>74</sup> function of the interatomic distance between atom  $A$  and atom  $B$ , which approximates the Hartree and (spin-unpolarized) exchange-correlation contributions from the charge fluctuations. The chosen form of  $\gamma$  depends on the quantities

$$U_{Al} = \frac{\partial \varepsilon_l}{\partial n_l}, \quad (\text{A10})$$

which can be considered as a generalization of the Hubbard model  $U$  values. In a similar way, writing the magnetization fluctuation compared to the unpolarized reference ( $\Delta m$ ) as sum of atomic contribution, in the framework of the monopole approximation, the term  $E_{\delta m}$  in Eq. (A3) can be written<sup>66</sup> as

$$E_{\delta m} = \frac{1}{2} \sum_A \sum_{l \in A} \sum_{l' \in A} \Delta m_{Al} \Delta m_{Al'} W_{All'}, \quad (\text{A11})$$

where the  $W_{ll'}$  are atomic constants defined as

$$W_{ll'} = \frac{1}{2} \left( \frac{\partial \varepsilon_{l\uparrow}}{\partial \varepsilon_{l'\uparrow}} - \frac{\partial \varepsilon_{l\downarrow}}{\partial \varepsilon_{l'\downarrow}} \right) \quad (\text{A12})$$

and the magnetization fluctuations in the Mulliken populations compared to the spin unpolarized reference system are

$$\Delta m_{Al} = \frac{1}{2} \sum_{i=1}^{\text{occ}} n_{i\sigma} \sum_{\mu \in A, l} \sum_{\nu} (c_{\mu i\uparrow}^* c_{\nu i\uparrow} S_{\mu\nu} - c_{\mu i\downarrow}^* c_{\nu i\downarrow} S_{\nu\mu}), \quad (\text{A13})$$

with the up and down coefficients labeled by arrows.

### 3. Repulsive contribution

The terms collected together as  $E_{\text{rep}}$  in Eq. (A3) are not calculated separately, although this is, in principle, possible, but merged into one repulsive pair potential  $U_{\text{rep}}(|\mathbf{R}_A - \mathbf{R}_B|)$ , in the spirit of empirical TB.<sup>75</sup> This potential only depends on atomic separation and species and is evaluated as the difference between the Kohn-Sham DFT total energy and the electronic part of the DFTB energy. For each chemical combination of atom pairs in our system, we have

$$U_{\text{rep}}(|\mathbf{R}_A - \mathbf{R}_B|) = E_{\text{tot}}^{KS}(|\mathbf{R}_A - \mathbf{R}_B|) - E_{\text{el}}^{\text{DFTB}}(|\mathbf{R}_A - \mathbf{R}_B|), \quad (\text{A14})$$

and the sum over all the atom pairs in the system gives the repulsive part of the energy:

$$E_{\text{rep}} = \frac{1}{2} \sum_{A, B} U_{\text{rep}}(|\mathbf{R}_A - \mathbf{R}_B|). \quad (\text{A15})$$

For each combination of atomic species, the pair repulsive potential  $U_{\text{rep}}(|\mathbf{R}_A - \mathbf{R}_B|)$  is calculated for a fit system in a chosen interval of interatomic separations and tabulated.

#### 4. Total energy and potential

The expression for the total energy within the spin-polarized DFTB approximation is then the sum of four contributions:

$$E_{tot} = \sum_{\sigma=\downarrow,\uparrow} \sum_i^{occ} n_{i\sigma} \langle \psi_{i\sigma} | \hat{H}_0[n_0, 0] | \psi_{i\sigma} \rangle + E_{\delta n} + E_{\delta m} + E_{rep}. \quad (A16)$$

The Hamiltonian operator of zeroth order depends only on the reference density, the second term on fluctuations in the Mulliken charges,  $\Delta q_{Al}$ , compared to the parametrizing reference system, the third from the spin polarization (through the Mulliken spin population  $\Delta m_{Al}$ ), and the fourth term, the repulsive potential  $E_{rep}$ , depends only on the atomic coordinates and species. Applying the variational principle to Eq. (A16) for the total energy, we get<sup>19,74</sup> a secular equation for the coefficients  $c_{vi\sigma}$  of the wave functions:

$$\sum_v c_{vi\sigma} (\hat{H}_{\mu\nu\sigma} - \varepsilon_{i\sigma} S_{\mu\nu}) = 0, \quad (A17)$$

with Hamiltonian matrix elements

$$\begin{aligned} \hat{H}_{\mu\nu\sigma} = & \hat{H}_{\mu\nu}^0 + \frac{1}{2} S_{\mu\nu} \sum_C^M \sum_{l'' \in C} (\gamma_{A(\mu)l(\mu), C l''} + \gamma_{B(\nu)l(\nu), C l''}) \Delta q_{cl''} \\ & + \delta_{\sigma} \frac{1}{2} S_{\mu\nu} \left( \sum_{l' \in B(\mu)} W_{B(\mu)l(\mu)l'} \Delta m_{B(\mu)l'} \right. \\ & \left. + \sum_{l' \in B(\nu)} W_{B(\nu)l(\nu)l'} \Delta m_{B(\nu)l'} \right) \end{aligned} \quad (A18)$$

and overlap matrix elements

$$S_{\mu\nu} = \langle \varphi_{\mu} | \varphi_{\nu} \rangle. \quad (A19)$$

Here, we have used the symbol  $\delta_{\sigma} = \pm 1$  for the up and down electrons, respectively. Note that this expression slightly differs from that reported in the earliest form of spin-resolved DFTB<sup>66</sup> as the one-center spin approximation in the potential has been dropped.<sup>76</sup> The Hamiltonian matrix elements in the Eq. (A18) depend, through the Mulliken spin populations, on the wave function coefficients  $c_{vi\sigma}$ ; therefore, the problem must be solved self-consistently.

\*s.sanna@phys.upb.de

<sup>1</sup>C. G. Duan, R. F. Sabiryanov, W. N. Mei, P. A. Dowben, S. S. Jaswal, and E. Y. Tsymlal, *J. Phys.: Condens. Matter* **19**, 315220 (2007).

<sup>2</sup>F. Aryasetiawan and O. Gunnarsson, *Rep. Prog. Phys.* **61**, 237 (1998).

<sup>3</sup>J. P. Perdew and A. Zunger, *Phys. Rev. B* **23**, 5048 (1981).

<sup>4</sup>A. Svane and O. Gunnarsson, *Phys. Rev. Lett.* **65**, 1148 (1990).

<sup>5</sup>B. Hourahine, B. Aradi, and T. Frauenheim (unpublished).

<sup>6</sup>T. Frauenheim *et al.*, *J. Phys.: Condens. Matter* **14**, 3015 (2002).

<sup>7</sup>D. Vogel, P. Krüger, and J. Pollmann, *Phys. Rev. B* **58**, 3865 (1998); **55**, 12836 (1997).

<sup>8</sup>A. Filippetti and N. A. Spaldin, *Phys. Rev. B* **67**, 125109 (2003).

<sup>9</sup>A. G. Petukhov, W. R. L. Lambrecht, and B. Segall, *Phys. Rev. B* **53**, 4324 (1996).

<sup>10</sup>S. Nishio, T. Nakagawa, T. Arakawa, N. Tomioka, T. A. Yamamoto, T. Kusunose, K. Niihara, T. Numazawa, and K. Kamiya, *J. Appl. Phys.* **99**, 08K901 (2006).

<sup>11</sup>T. Nakagawa, T. Arakawa, K. Sako, N. Tomioka, T. A. Yamamoto, T. Kusunose, K. Niihara, K. Kamiya, and T. Numazawa, *J. Alloys Compd.* **408**, 191 (2006).

<sup>12</sup>A. J. Steckl, J. Heikenfeld, D. S. Lee, and M. Garter, *Mater. Sci. Eng., B* **B81**, 97 (2001).

<sup>13</sup>G. M. Dalpian and Su-Huai Wei, *Phys. Rev. B* **72**, 115201 (2005).

<sup>14</sup>S. Dhar, O. Brandt, M. Ramsteiner, V. F. Sapega, and K. H. Ploog, *Phys. Rev. Lett.* **94**, 037205 (2005).

<sup>15</sup>M. Haugk *et al.*, *Phys. Status Solidi B* **217**, 473 (2000).

<sup>16</sup>M. Elstner, Th. Frauenheim, E. Kaxiras, G. Seifert, and S. Suhai, *Phys. Status Solidi B* **217**, 375 (2000).

<sup>17</sup>A. Sieck, Ph.D. thesis, Universität Paderborn, 2001.

<sup>18</sup>E. Rauls, Ph.D. thesis, Universität Paderborn, 2003.

<sup>19</sup>D. Porezag, Th. Frauenheim, Th. Köhler, G. Seifert, and R.

Kaschner, *Phys. Rev. B* **51**, 12947 (1995).

<sup>20</sup>J. Widany, Th. Frauenheim, Th. Köhler, M. Sternberg, D. Porezag, G. Jungnickel, and G. Seifert, *Phys. Rev. B* **53**, 4443 (1996).

<sup>21</sup>J. Elsner, R. Jones, M. I. Heggie, P. K. Sitch, M. Haugk, Th. Frauenheim, S. Oberg, and P. R. Briddon, *Phys. Rev. B* **58**, 12571 (1998).

<sup>22</sup>J. Elsner, M. Haugk, J. Jungnickel, and Th. Frauenheim, *J. Mater. Chem.* **6**, 1649 (1996).

<sup>23</sup>A. I. Liechtenstein, V. I. Anisimov, and J. Zaanen, *Phys. Rev. B* **52**, R5467 (1995).

<sup>24</sup>C. Köhler, G. Seifert, and Th. Frauenheim, *Chem. Phys.* **309**, 23 (2005).

<sup>25</sup>O. A. Vydrov, G. E. Scuseria, J. P. Perdew, A. Ruzsinszky, and G. I. Csonka, *J. Chem. Phys.* **124**, 094108 (2006).

<sup>26</sup>V. I. Anisimov, F. Aryasetiawan, and A. I. Liechtenstein, *J. Phys.: Condens. Matter* **9**, 767 (1997).

<sup>27</sup>M. T. Czyżyk and G. A. Sawatzky, *Phys. Rev. B* **49**, 14211 (1994).

<sup>28</sup>V. I. Anisimov, I. V. Solovyev, M. A. Korotin, M. T. Czyżyk, and G. A. Sawatzky, *Phys. Rev. B* **48**, 16929 (1993).

<sup>29</sup>A. G. Petukhov, I. I. Mazin, L. Chioncel, and A. I. Liechtenstein, *Phys. Rev. B* **67**, 153106 (2003).

<sup>30</sup>D. A. Papaconstantopoulos and C. S. Hellberg, *Phys. Rev. Lett.* **89**, 029701 (2002).

<sup>31</sup>S. L. Dudarev, G. A. Botton, S. Y. Savrasov, C. J. Humphreys, and A. P. Sutton, *Phys. Rev. B* **57**, 1505 (1998).

<sup>32</sup>M. J. Han, T. Ozaki, and J. Yu, *Phys. Rev. B* **73**, 045110 (2006).

<sup>33</sup>C. D. Pemmaraju, T. Archer, D. Sanchez-Portal, and S. Sanvito, *Phys. Rev. B* **75**, 045101 (2007).

<sup>34</sup>J. P. Perdew and M. Levy, *Phys. Rev. Lett.* **51**, 1884 (1983).

<sup>35</sup>L. J. Sham and M. Schlüter, *Phys. Rev. Lett.* **51**, 1888 (1983).

<sup>36</sup>C. M. Aerts, P. Strange, M. Horne, W. M. Temmerman, Z. Szotek,

- and A. Svane, Phys. Rev. B **69**, 045115 (2004).
- <sup>37</sup>Z. Szotek, W. M. Temmerman, A. Svane, L. Petit, P. Strange, G. M. Stocks, D. Ködderitzsch, W. Hergert, and H. Winter, J. Phys.: Condens. Matter **16**, S5587 (2004).
- <sup>38</sup>C. G. Duan, R. F. Sabiryanov, J. Liu, W. N. Mei, P. A. Dowben, and J. R. Hardy, J. Appl. Phys. **97**, 10A915 (2005).
- <sup>39</sup>G. Busch, P. Junod, O. Vogt, and F. Hulliger, Phys. Lett. **6**, 79 (1963).
- <sup>40</sup>O. Vogt and K. Mattenberger, J. Alloys Compd. **223**, 226 (1995).
- <sup>41</sup>Ralph W. G. Wyckoff, *Crystal Structures* (Krieger, Malabar, FL, 1982), Vol. 1.
- <sup>42</sup>W. M. Temmerman, Z. Szotek, A. C. Jenkins, A. Svane, H. Winter, S. V. Beiden, and G. A. Gehring, in *Magnetism and Electronic Correlations in Local Moment Systems: Rare Earth Elements and Compounds*, edited by M. Donath, P. A. Dowben, and W. Nolting, Proceedings of Magnetism and Electronic Correlations in Local-Moment Systems: Rare-Earth Elements and Compounds, Berlin, Germany, 1998 (World Scientific, Singapore, 1998), pp. 21–33.
- <sup>43</sup>H. J. Monkhorst and J. D. Pack, Phys. Rev. B **13**, 5188 (1976).
- <sup>44</sup>B. Hourahine, S. Sanna, B. Aradi, C. Köhler, and Th. Frauenheim, Physica B **376**, 512 (2006).
- <sup>45</sup>Z. Huang, L. Ye, Z. Q. Yang, and X. Xie, Phys. Rev. B **61**, 12786 (2000).
- <sup>46</sup>J.-S. Filhol, R. Jones, M. J. Shaw, and P. R. Briddon, Appl. Phys. Lett. **84**, 2841 (2004).
- <sup>47</sup>P. Dorembos and E. van der Kolk, Appl. Phys. Lett. **89**, 061122 (2006).
- <sup>48</sup>A. Svane, N. E. Christensen, L. Petit, Z. Szotek, and W. M. Temmerman, Phys. Rev. B **74**, 165204 (2006).
- <sup>49</sup>J. T. Torvik, R. J. Feuerstein, J. I. Pankove, C. H. Qiu, and F. Namavar, Appl. Phys. Lett. **69**, 2098 (1996).
- <sup>50</sup>P. H. Citrin, P. A. Northrup, R. Birckhahn, and A. J. Steckl, Appl. Phys. Lett. **76**, 2865 (2000).
- <sup>51</sup>D. S. Lee, J. Heikenfeld, R. Birkhan, M. Garter, B. K. Lee, and A. J. Steckl, Appl. Phys. Lett. **76**, 1525 (2000).
- <sup>52</sup>A. J. Steckl, J. Heikenfeld, D. S. Lee, and M. Garter, Mater. Sci. Eng., B **81**, 97 (2001).
- <sup>53</sup>J. M. Zavada, S. X. Jin, N. Nepal, J. Y. Lin, H. X. Jiang, P. Chow, and B. Hertog, Appl. Phys. Lett. **84**, 1061 (2004).
- <sup>54</sup>M. Thaik, U. Hömmerich, R. N. Schwartz, R. G. Wilson, and J. M. Zavada, Appl. Phys. Lett. **71**, 2641 (1997).
- <sup>55</sup>S. F. Song, W. D. Chen, J. Zhu, and C. C. Hsu, J. Cryst. Growth **265**, 78 (2004).
- <sup>56</sup>U. Wahl, E. Alves, K. Lorenz, J. G. Correia, T. Monteiro, B. de Vries, A. Vantomme, and R. Vianden, Mater. Sci. Eng., B **105**, 132 (2003).
- <sup>57</sup>V. Glukhanyuk, H. Przybylińska, A. Kozanecki, and W. Lantsch, Phys. Status Solidi A **201**, 195 (2004).
- <sup>58</sup>V. Katchkanov, J. F. W. Mosselmans, K. P. O'Donnel, E. Nogales, S. Hernandez, R. W. Martin, A. J. Stekl, and D. S. Lee, Opt. Mater. (Amsterdam, Neth.) **28**, 785 (2006).
- <sup>59</sup>S. Sanna, B. Hourahine, Th. Gallauner, and Th. Frauenheim, J. Phys. Chem. A **111**, 5671 (2007).
- <sup>60</sup>H. Bang, S. Morishima, Z. Li, K. Akimoto, M. Nomura, and E. Yagi, J. Cryst. Growth **237-239**, 1027 (2002).
- <sup>61</sup>P. Blaha, K. Schwarz, G. Madsen, D. Kvasnicka, and J. Luitz, WIEN2K, Institute of Materials Chemistry, TU Vienna.
- <sup>62</sup>K. P. O'Donnell, and B. Hourahine, Eur. Phys. J.: Appl. Phys. **36**, 91 (2006).
- <sup>63</sup>M. Kotzian, N. Rösch, and M. C. Zerner, Theor. Chim. Acta **81**, 201 (1992).
- <sup>64</sup>U. von Barth and L. Hedin, J. Phys. C **5**, 1629 (1972).
- <sup>65</sup>W. Kohn and L. P. Sham, Phys. Rev. **140**, A1133 (1965).
- <sup>66</sup>T. Frauenheim, G. Seifert, M. Elstner, Z. Hajnal, G. Jungnickel, D. Porezag, S. Shuai, and R. Scholz, Phys. Status Solidi B **217**, 41 (2000).
- <sup>67</sup>V. Heera, G. Seifert, and P. Ziesche, J. Phys. B **17**, 519 (1984).
- <sup>68</sup>Hence giving the correct limiting case for isolated atoms.
- <sup>69</sup>Since the basis functions decay in space, above a certain distance ( $r_{\text{cutoff}}$ ), their matrix elements are then smaller than a reasonable tolerance, and these elements are then discarded. Note that the potential in Eq. (A6) is a superposition of the atomic potentials. Another possibility is to express it as the potential generated by the superposition of the charge densities of *A* and *B*, as is used instead in some DFTB parametrizations (Ref. 74).
- <sup>70</sup>J. C. Slater and G. F. Koster, Phys. Rev. **94**, 1498 (1954).
- <sup>71</sup>K. Lendi, Phys. Rev. B **9**, 2433 (1974).
- <sup>72</sup>A. V. Podolskiy and P. Vogl, Phys. Rev. B **69**, 233101 (2004).
- <sup>73</sup>Unlike empirical tight binding, however, since an explicit basis set is used in the generation of parameters, it is also possible to plot the resulting single-particle wave functions or the total “charge density” (see Fig. 4, for example).
- <sup>74</sup>M. Elstner, D. Porezag, G. Jungnickel, J. Elsner, M. Haugk, T. Frauenheim, S. Suhai, and G. Seifert, Phys. Rev. B **58**, 7260 (1998).
- <sup>75</sup>D. J. Chadi, Phys. Rev. Lett. **43**, 43 (1979).
- <sup>76</sup>C. Köhler, G. Seifert, and Th. Frauenheim, Chem. Phys. **23**, 309 (2005).
- <sup>77</sup>C. Köhler, B. Hourahine, G. Seifert, M. Sternberg, and T. Frauenheim, J. Phys. Chem. A **111**, 5622 (2007).